Large amplitude electrostatic proton plasma frequency waves in the magnetospheric separatrix and outflow regions during magnetic reconnection

K. Steinvall[1,2], Yu. V. Khotyaintsev[1], D. B. Graham[1], A. Vaivads[3], M. André[1], C. T. Russell[4]

[1]Swedish Institute of Space Physics, Uppsala, Sweden
[2]Space and Plasma Physics, Department of Physics and Astronomy, Uppsala University, Uppsala, Sweden
[3]Division of Space and Plasma Physics, School of Electrical Engineering and Computer Science, KTH Royal Institute of Technology, Stockholm, Sweden
[4]Institute of Geophysics and Planetary Physics, University of California, Los Angeles, CA, USA

Key Points:

- Large amplitude electrostatic waves are found in the magnetospheric separatrix region
- The waves are driven by an ion acoustic instability due to the presence of cold ions
- The ion acoustic waves may heat cold magnetospheric ions and dissipate parallel currents

Corresponding author: Konrad Steinvall, `konrad.steinvall@irfu.se`

Abstract

We report Magnetospheric Multiscale observations of large amplitude, parallel, electrostatic, proton plasma frequency waves on the magnetospheric side of the reconnecting magnetopause. The waves are often found in the magnetospheric separatrix region and in the outflow near the magnetospheric ion edge. Statistical results from five months of data show that these waves are closely tied to the presence of cold (typically tens of eV) ions, found for 88% of waves near the separatrix region, and that plasma properties are consistent with ion acoustic wavegrowth. We analyze one wave event in detail, concluding that the wave is ion acoustic. We provide a simple explanation for the mechanisms leading to the development of the ion acoustic instability. These waves can be important for separatrix dynamics by heating the cold ion component and providing a mechanism to damp the kinetic Alfvén waves propagating away from the reconnection site.

Plain Language Summary

The magnetopause is the magnetic boundary shielding the Earth's magnetosphere from the shocked solar wind plasma of the magnetosheath. Magnetic reconnection, a fundamental plasma process, locally breaks this boundary, leading to energization and mixing of magnetospheric and solar wind plasma. During the reconnection process, the plasma is highly unstable and many different kinds of waves appear. In this Letter we investigate the large amplitude electrostatic waves with frequencies around the proton plasma frequency which are often found in spacecraft observations of magnetic reconnection. We find that the waves can appear when cold (tens of eV) magnetospheric ions are present at the magnetopause, and are generated by an ion acoustic instability between the cold ions and the fast flowing electrons often observed during magnetic reconnection. The waves might heat the cold ions and couple to the large scales by dissipating parallel currents.

1 Introduction

The magnetopause is the boundary between the Earth's magnetosphere and the shocked solar wind plasma of the magnetosheath. Plasma waves are often found in the vicinity of the magnetopause (e.g. Fairfield, 1976; Gurnett et al., 1979; LaBelle et al., 1987; Tang et al., 2019), and appear to be intimately connected to magnetic reconnection (Khotyaintsev et al., 2019), a fundamental plasma process where changes in magnetic field topology result in plasma mixing and explosive energy conversion from magnetic energy to kinetic and thermal energy (e.g. Birn & Priest, 2007). Though magnetic reconnection is a well studied subject some fundamental aspects are still not understood, and studying wave dynamics might be crucial to fully understand the cause and effects of magnetic reconnection (Khotyaintsev et al., 2019; Wilder et al., 2019).

The separatrix region is defined as the kinetic boundary separating the inflow and outflow regions of magnetic reconnection (Lindstedt et al., 2009). As such, this region is characterized by recently reconnected magnetic field lines, complex distribution functions, and large parallel currents (Khotyaintsev et al., 2006) likely associated with kinetic Alfvén waves propagating away from the reconnection site (Dai et al., 2017; Dai, 2018; Huang et al., 2018). At the reconnecting dayside magnetopause, which is the focus of this Letter, the complexity is even greater due to the variable plasma composition. Here the typically tenuous magnetosphere, which can contain both hot (~ 1 keV) and cold (~ 10 eV) plasma (André & Cully, 2012; Lee & Angelopoulos, 2014), is mixing with the dense ~ 100 eV magnetosheath plasma. The end result is that the plasma is unstable to the generation of various waves which are often found in spacecraft observations. Examples include beam and loss cone driven whistler waves (Graham, Vaivads, et al., 2016; Uchino et al., 2017), electron holes (Farrell et al., 2002; Graham et al., 2015; Holmes et al., 2019), Langmuir waves (Vaivads et al., 2004; Wilder et al., 2016; Zhou et al., 2016), ion acoustic waves (Uchino et al., 2017), and electron acoustic waves (Ergun, Holmes, et al., 2016).

Early observations from the Magnetospheric Multiscale (MMS) mission (Burch et al., 2016) reported the presence of electrostatic waves with large amplitude parallel (to the magnetic field) electric fields ($E_{\parallel}$) in the magnetospheric separatrix region close to the electron diffusion region (Ergun, Holmes, et al., 2016). The waves were found with frequencies both below and significantly above the ion plasma frequency f_{pi}. By comparing observations with simulations, the high frequency waves were argued to be consistent with electron acoustic waves driven by the interaction of a cold magnetospheric electron beam with a warmer electron beam of magnetosheath origin, while the mechanism behind the lower frequency waves observed in the MMS data could not be determined unambiguously. Uchino et al. (2017) used Time History of Events and Macroscale Interactions during Substorms (THEMIS) (Angelopoulos, 2008) data to investigate waves found in the innermost open boundary layer during dayside magnetopause reconnection. The authors presented one wave event similar to the low frequency waves found by Ergun, Holmes, et al. (2016) and concluded that the wave was generated by an ion acoustic instability. However, to the best of our knowledge, no statistical study of these low frequency waves has yet been published.

In this Letter we use data from MMS to study the large amplitude, electrostatic, ion plasma frequency waves observed in and around the magnetospheric separatrix region during ongoing magnetic reconnection, looking to answer the questions: What is the instability generating these waves? What effect do these wave have on the separatrix plasma dynamics?

2 Wave observation example

In this section we start by discussing large amplitude waves observed by MMS during a crossing of the reconnecting magnetopause on the 24th of October 2015. The waves are similar to the low frequency waves reported by Ergun, Holmes, et al. (2016) in that they are electrostatic, have large $E_{\|}$, nonlinear waveforms, and frequencies close to f_{pi}. We then analyze one wave in detail, placing it in the context of magnetic reconnection, and determine its generation mechanism and effect on the plasma dynamics.

We present an overview of this magnetopause crossing in Fig. 1. This event has previously been analyzed in the context of reconnection in the presence of cold ions by Toledo-Redondo et al. (2017). Initially, MMS is located in the magnetosphere. At around 07:03:48 UT, highlighted by the red shaded area, MMS crosses the electron edge (Gosling et al., 1990; Lindstedt et al., 2009) as seen by the sudden appearance of low energy magnetosheath electrons and reduction of high energy magnetospheric electrons (Fig. 1b). Shortly after, around 07:03:51, MMS crosses the ion edge (green shaded region) where the first ions of magnetosheath origin are observed (Fig. 1c) and enters the outflow region while remaining close to the ion edge. During this time, strong parallel currents are observed $j_{\|} \approx$ 500 nA/m^2 (Fig. 1f), together with waves (Fig. 1g) with amplitudes reaching up to 200 mV/m. There are no corresponding magnetic field fluctuations (not shown), meaning the waves are electrostatic. The frequencies of the waves are slightly below f_{pi} (Fig. 1h), which indicates that ion dynamics are likely to play a role in the generation mechanism.

In order to investigate the generation mechanism and understand how these waves interact with the plasma, we zoom in to the large amplitude waves marked by the dashed

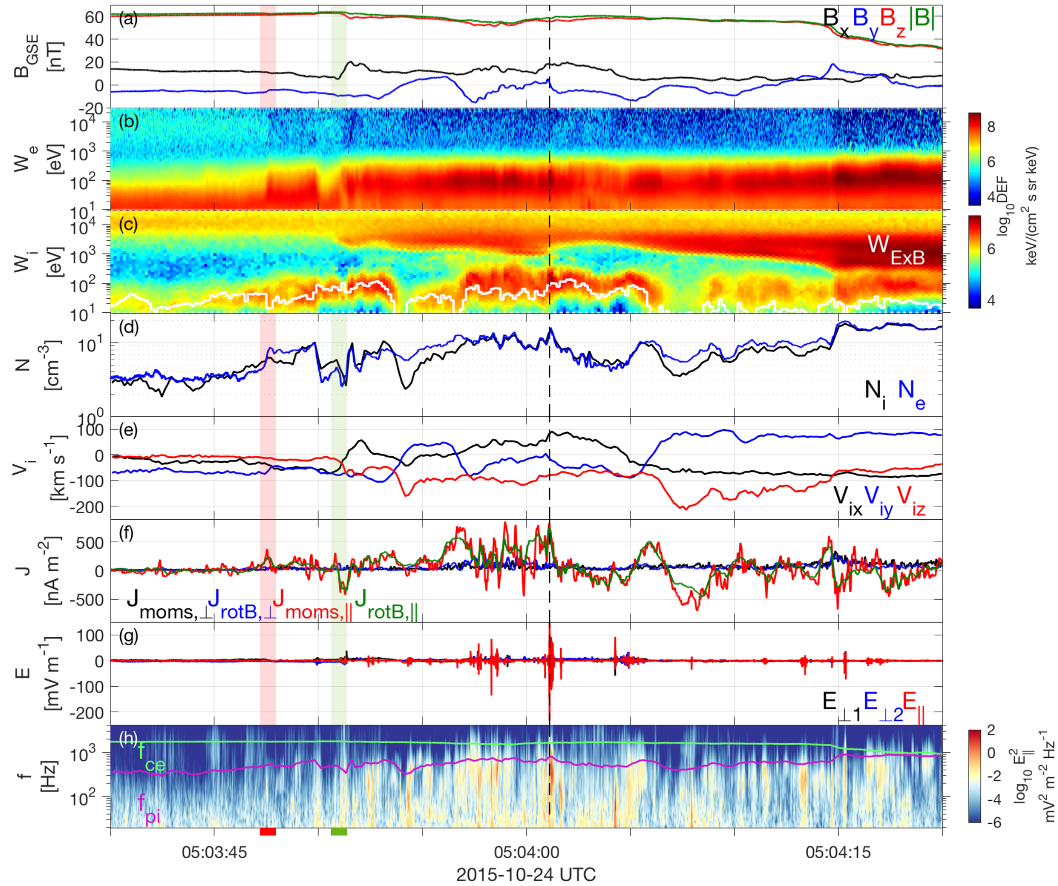

Figure 1. Overview of wave observation from MMS4. (a) Magnetic field data from the Flux-gate magnetometer (Russell et al., 2016) in geocentric solar ecliptic (GSE) coordinates. (b,c) Differential energy flux (DEF) from Fast Plasma Investigation (FPI) (Pollock et al., 2016) for electrons and ions. The white line in (c) is the energy corresponding to the $\mathbf{E} \times \mathbf{B}$ drift. (d) Ion and electron density from FPI. The deviation from quasi-neutrality is artificial, mainly due to cold ions with energies below FPI's energy threshold. (e) Ion velocity from FPI in GSE. (f) Currents in magnetic field aligned coordinates (FAC) calculated using $\nabla \times \mathbf{B}$ and FPI plasma moments. (e) Electric field from the Electric field Double Probes (EDP) (Lindqvist et al., 2016; Ergun, Tucker, et al., 2016) in FAC. (h) Spectral power density of $E_{\|}$. The green(purple) line corresponds to the electron cyclotron(ion plasma) frequency. The verical red and green bars show approximately the location of the electron and ion edges.

vertical line in Fig. 1, and plot the 1 and 2-dimensional velocity distribution functions (VDFs) for ions (Figs. 2a,f-h) and electrons (Figs. 2b,i-k). The VDFs have been integrated over the entire velocity range of FPI. In the case of ions, two components are clearly visible. The cold component with $v_{\|} \approx -20$ km/s corresponds to the cold magnetospheric ions seen in Fig. 1c whereas the hotter component with $v_{\|} \approx -500$ km/s and the characteristic D-shape in Fig. 2f corresponds to transmitted magnetosheath ions moving along reconnected field lines south of the x-line (Cowley, 2013), consistent with the southward ion outflow in Fig. 1e. The gradual disappearance of low speed magnetosheath ions starting after ~05:04:01 in Fig. 2a indicates that the spacecraft is moving closer to the magnetospheric ion edge. The electron VDF primarily contains magnetosheath electrons, and is slightly shifted in the $-v_{\|}$ direction, corresponding to the positive $j_{\|}$ in Fig. 1f. The different plasma components and their distinct parallel bulk velocities constitute a system where there are several positive slopes in the VDFs, and Landau resonance could lead to spontaneous growth of different waves.

Before moving on to dispersion analysis, we briefly discuss the electrostatic properties of the wave shown in Figs. 2c-e. In particular we want to determine the wave's phase velocity $\boldsymbol{v}_\phi = v_\phi \hat{\boldsymbol{k}}$ for two reasons. The first reason is that v_ϕ depends on the generation mechanism, and thus serves as a diagnostic to determine what instability generated the wave. The second reason is that once v_ϕ is known, the electrostatic potential can be calculated as $\Phi = \int \delta E v_\phi dt$. In this case we are particularly interested in Φ since the waveform of δE is non-linear, raising two questions which require Φ to answer: Is there a net potential change $\Delta\Phi$ associated with the waves? Is the non-linear waveform due to electron or ion trapping? Since the wave is electrostatic and linearly polarized, $\boldsymbol{k} \times \delta\mathbf{E} = 0$, and we can determine $\hat{\boldsymbol{k}}$ using maximum variance analysis of $\delta\mathbf{E}$. We find that $\pm\hat{\boldsymbol{k}}$ is field aligned within the uncertainty. We determine v_ϕ and the sign of $\hat{\boldsymbol{k}}$ using cross-spectral analysis of the electric field between the axial EDP probes (Graham, Khotyaintsev, et al., 2016) and obtain $v_\phi \approx -100$ km/s. Due to the short baseline of the axial EDP probes, this speed should be interpreted only as a rough estimate of the actual phase speed. The sign, implying anti-parallel propagation, is determined with much greater confidence. The slow v_ϕ indicates that the instability generating this wave is most likely an interaction between either the two ion components, or the cold ions and the electrons. We calculate Φ with $\delta\mathbf{E}$ high-pass filtered at 100Hz and plot the results in Fig. 2d. We conclude that there is no significant potential change across the waves, $\Delta\Phi = 0$, and

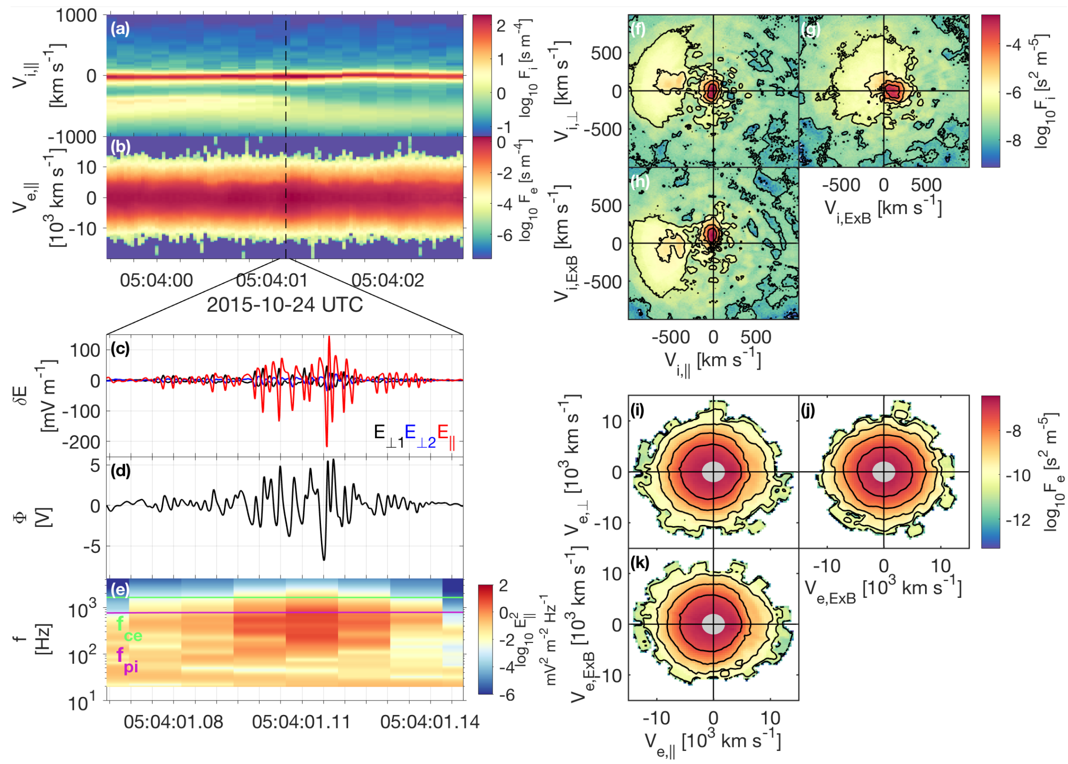

Figure 2. Particle distribution functions and wave properties observed by MMS4. (a,b) 1-dimensional ion and electron velocity distribution functions (VDFs). (c) Waveform of **E** high-pass filtered at 100 Hz. (d) Electrostatic potential of the wave. (e) Spectral power density of $E_\parallel$. (f-h) 2-dimensional VDFs of ions sampled at 05:04:01.078. (i-k) 2-dimensional VDFs of electrons sampled at 05:04:01.108, marked by the vertical dashed line in panels (a) and (b). The central area of the 2-dimensional electron VDFs corresponding to energies not resolved by FPI are blocked out.

that the peak value of around $\Phi = 5$V corresponds to an ion trapping range $v_{tr,i} = v_\phi \pm \sqrt{2e\Phi/m_i}$ of around $(-130, -70)$ km/s, and equivalently an electron trapping range of around $(-1400, 1200)$ km/s in the spacecraft frame. The waves are thus capable of trapping parts of both the cold ion and electron components, which for example might lead to heating of the cold ions and local flattening of the electron VDF.

We are now in a position to set up and solve the one-dimensional electrostatic dispersion relation (Fried & Conte, 1961)

$$D(\omega, k) = 0 = 1 + \chi_{i,\text{cold}} + \chi_{i,\text{beam}} + \chi_{i,\text{bg}} + \chi_e, \tag{1}$$

where $\chi_s(\omega, k)$ is the susceptibility of plasma component s. In addition to the plasma components we discussed previously, we include a hot background ion component $\chi_{i,\text{bg}}$, corresponding to the hot magnetospheric ions in Fig. 1c. In Fig. 3a we show the observed reduced 1-dimensional VDFs for ions and electrons as the gray circles and cyan triangles respectively, and the Maxwellian fits by the solid lines. For the fits, we used the densities (units of cm^{-3}) $n_{i,\text{cold}} = 11.076$, $n_{i,\text{beam}} = 0.48$, $n_{i,\text{bg}} = 0.08$, $n_e = 11.636$, thermal speeds (in km/s): $v_{th;i,\text{beam}} = 180$, $v_{th;i,\text{cold}} = 35$, $v_{th;i,\text{bg}} = 900$, $v_{th;e} = 4160$, and parallel drift speeds (in km/s): $v_{d;i,\text{cold}} = 20$, $v_{d;i,\text{beam}} = -580$, $v_{d;i,\text{bg}} = -330$, $v_{d;e} = -410$. The corresponding temperature ratio between the cold ions and the electrons is $T_{i,\text{cold}}/T_e \approx 0.13$. Solving Eq. (1) numerically we find positive wavegrowth for the solution in Fig. 3b. The black(red) line corresponds to the real(imaginary) frequency $\omega(\gamma)$, and the circles mark the point of largest γ. The negative ω implies propagation in the anti-parallel direction, as was found in observations, and the phase speed at maximum growth marked by the dashed line in Fig. 3a is $v_{\max(\gamma)} = -102$ km/s, close to the observed v_ϕ. $v_{\max(\gamma)}$ coincides with a positive slope of the drifting electron VDF, thus driving the wave via Landau resonance. In Fig. 3c, we plot the real part of the different χ_s and confirm that the wave is due to the electrons and cold ions. The imaginary parts of χ_s (not shown) show similar results. The ion-ion instability is stabilized by the electrons in this case. We thus conclude that an ion acoustic instability is the source behind the observed waves.

In summary, for this event we find $E_\parallel$ waves with frequency close to f_{pi} in the reconnection outflow, near the magnetospheric ion edge. The analyzed wave is propagating slowly ($v_\phi \approx 100$ km/s) in the anti-parallel direction, carries no $\Delta\Phi$, and can trap parts of the electron and cold ion distributions. Dispersion analysis shows that the plasma

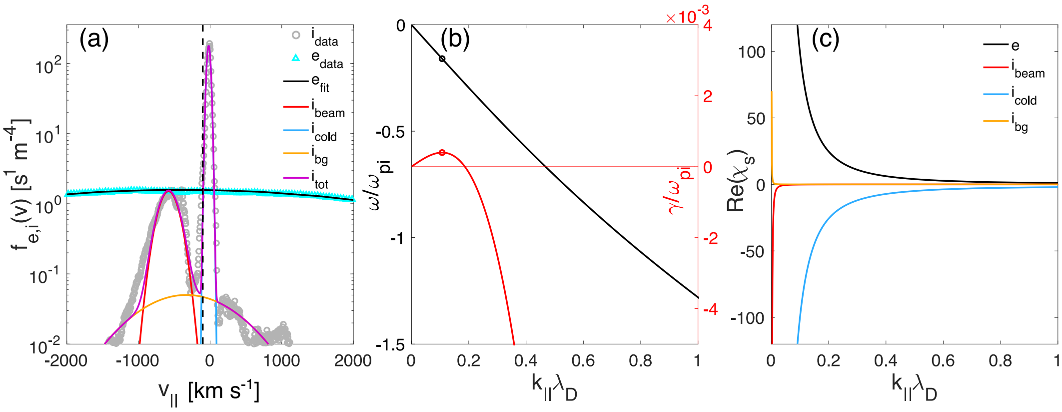

Figure 3. Dispersion analysis. (a) Observed and fitted reduced VDFs. The dashed line corresponds to the phase speed of the fastest growing wave. (b) Dispersion relation. The circles mark the points corresponding to the highest growth rate, and λ_D is the Debye length. (c) Real part of the susceptibilities of the plasma components for the solution in (b).

is unstable to an ion acoustic instability between the dominating cold ions and the drifting electrons.

3 Statistics

Armed with the knowledge from the previous section, we would like to see if the ion acoustic instability can explain the wave observations on a statistical level. To investigate this, we scan through 5 months of MMS data when MMS is close to the dayside magnetopause (September through November 2015, and October through November 2016), searching for magnetopause crossings where waves with $E_{||} > 20$ mV/m and maximum power within the frequency band $[0.5, 2]f_{pi}$ are observed on the magnetospheric side. We find that when the waves are observed in the separatrix region and near the ion edge, cold ions are present for 88% (250/283) of the events. The waves where no cold ions are present tend to be either solitary waves or have a very small number of wave periods, and we exclude these from the following analysis. The wavevectors are typically close to field aligned, with a median wave normal angle of 16°. The waveforms are often nonlinear, as previously reported by Ergun, Holmes, et al. (2016). We are unfortunately not able to determine v_ϕ on a statistical level, only for 20 waves. This is primarily because B_z is generally the dominant magnetic field component, and the axial EDP probes are not ideal for interferometry due to their short separation and floating poten-

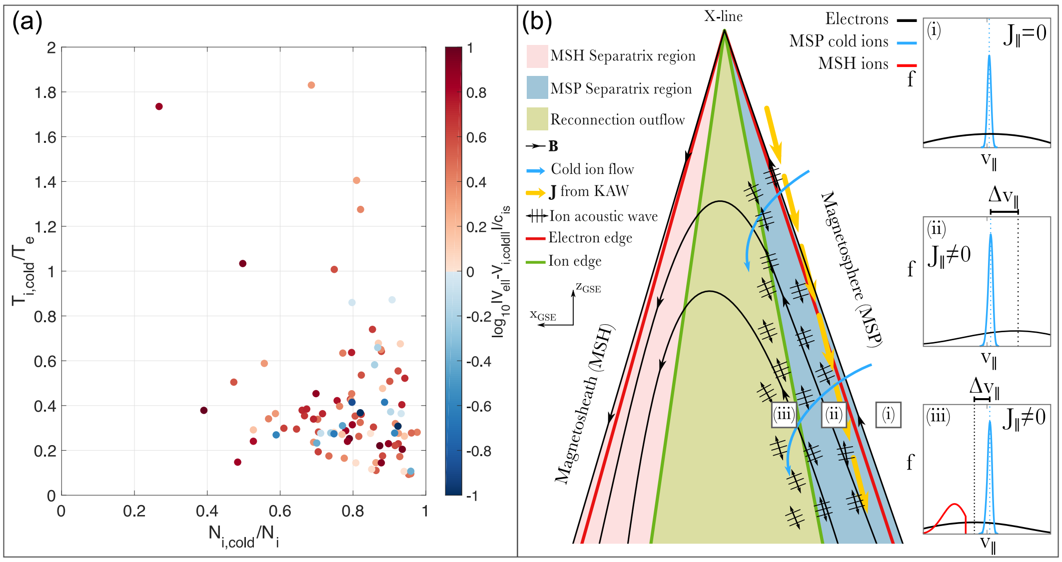

Figure 4. (a) Cold plasma properties for waves observed in the magnetospheric separatrix region and near the ion edge. (b) Illustration showing where in the reconnection picture the ion acoustic waves are observed and the process leading to their formation. The boxes (i), (ii), and (iii) show where the distribution functions in the right column are observed. The separatrices are the outermost drawn field lines.

tial difference compared to the spin-plane probes used to calculate the spacecraft potential (Graham et al., 2015). However, when we are able to roughly estimate v_ϕ it is typically small $\sim$ 100 km/s, similar to the example in Fig. 2. Since cold ions are present during most wave observations they are most likely essential for the generation mechanism, motivating a statistical investigation into the plasma composition. In order to easily compute the moments of the cold ion component we take the wave events where the energy, $W_{E\times B}$, corresponding to the $\mathbf{E}\times\mathbf{B}$ drift is close to the differential energy flux peak of the cold ions. We then compute the cold ion moments by integrating the distribution function from the lowest energy to $3W_{E\times B}$ to ensure that we capture the whole cold ion distribution and ignore any hot plasma. We only do this calculation when there is a clear energy separation between different ion components, resulting in 97 events gathered from 21 different orbits. In Fig. 4a we present the results. There is a clear trend that these waves are primarily found when the cold ions dominate $n_{i,\text{cold}}/n_i \gtrsim 0.6$, the cold ion temperature is much smaller than the electron temperature $T_{i,\text{cold}}/T_e \lesssim 0.4$, and when the parallel drift between the cold ions and electrons is near or greater than the ion sound speed c_{is}. These features are consistent with the ion acoustic instability which, in the simple model of a two component plasma, requires $T_i < T_e$ to avoid ion Landau damping, and energy for wavegrowth is provided by the drifting electrons (Baumjohann & Treumann, 1996; Stringer, 1964). What about the waves where we cannot compute the cold ion moments? We typically observe many wave events during each magnetopause crossing, but we can only apply our analysis on a few (the fraction in Fig. 4a). This is often because $W_{E\times B}$ fluctuates while the ion energy is comparitively unchanged. However, the waves have similar properties and the cold ion component is visually identifiable throughout the crossings. This suggests that the results in Fig. 4a likely apply to a larger set of waves, and that the same instability is likely responsible for most of the waves observed nearby.

Here we limited ourselves to waves found in the magnetospheric separatrix region and near the ion edge. This is because the inclusion of magnetosheath ions often makes it difficult to isolate the cold ion component (Li et al., 2017). Furthermore, as we go deeper into the jet and magnetosheath, similar waves start to appear independently of the presence of cold ions, suggesting another mechanism such as the ion-ion acoustic instability (Gary & Omidi, 1987) may be partly responsible for waves observed there.

4 Discussion

With this Letter we aimed at answering two main questions regarding the large amplitude electrostatic waves with frequencies near f_{pi} which MMS often observes at the reconnecting magnetopause. What is their generation mechanism? How do they affect the plasma?

Regarding the generation mechanism, there are three main pieces of evidence that, when combined, strongly points to the ion acoustic instability as the culprit. The first piece is the fact that the waves seem to be strongly connected to the ion scales, having frequencies around f_{pi}, and phase speeds in the range of the ion thermal speed. This suggests that an electron-electron instability is unlikely to be the source, and that ions are important. The second piece is the fact that 250 of 283 waves are found when cold ions are present. Moreover, for the 97 waves where we can easily compute the cold ion moments we find that cold ions are dominating and have temperatures well below the electron temperature, giving a strong indication that the cold plasma component is essential. The third piece is the fact that for the example event in Fig. 2, Eq. (1) predicts a growing ion acoustic wave. It is important to note that due to the dynamic nature of the separatrix region, the electron flow is highly variable (as seen by the currents in Fig. 1f), and waves that are growing in one instance of time may be stable or even damped in the next, also consistent with the localized, patchy, waveforms observed. This is reflected in the large variation of speeds shown in Fig. 4a. One result of this is that waves are frequently observed in plasma where the waves should be either marginally stable or slightly damped according to the numerical dispersion analysis. These electron variations, and the fact that the VDFs are not Maxwellian (contrary to the Maxwellianity assumption used in the analytical model) but often much more complex, makes a direct comparison between theory and observation difficult and not conclusive. However, these observations combined lets us conclude that the ion acoustic instability is very likely the source of these waves.

To answer the second question, regarding the effect of the waves, we need to take a step back and put the information into the context of magnetic reconnection. For the ion acoustic instability, the source of the free energy is the fast electron flow, which corresponds to the large $j_\parallel$ observed in the separatrix region. The underlying mechanism leading to the formation of $j_\parallel$ is the dynamics of a kinetic Alfvén wave (KAW) propagating away from the x-line (Vaivads et al., 2010; Huang et al., 2018; Dai, 2018). For the event in Fig. 1 there is evidence of KAW-dynamics. Starting from near the electron edge crossing and continuing until the end of the plot, there is a clear correlation between v_{ix} and B_x, and between v_{iy} and B_y. At the time where we see the strongest waves (dashed line), there is a peak in $j_\parallel$ associated with a B_y change of -12nT and an E_x increase of 3mV/m. The field ratio E_x/B_y corresponds to 0.8 times the local Alfvén speed ($v_A \approx$ 320 km/s), and the corresponding Poynting vector **S** is directed away from the x-line. These features are consistent with KAWs propagating away from the x-line (Shay et al., 2011; Huang et al., 2018). Analysing other field perturbations for this event yields similar conclusions. The effect of the instability is thus to dissipate $j_\parallel$ and damp KAWs. If the current dissipation is effective we expect $j_\parallel$ to approach the threshold value of the ion acoustic instability, which is $|j| \sim enc_{is}$ in the simple case of a two component plasma with $T_i \ll T_e$ (Stringer, 1964). In a more realistic scenario the waves will change the shape of the electron distribution and reduce the positive slope, likely leaving an average speed above c_{is} also at instability saturation. This picture is consistent with the observed current densities $|j| \approx 2 - 4enc_{is}$. Thus, the observation is consistent with the idea that the ion acoustic instability limits the current to the threshold value. The instability can thus effectively damp the KAWs propagating from the reconnection site to the ionosphere, thereby providing a coupling between Debye and larger scale physics.

Observations of ion acoustic waves during ongoing magnetic reconnection has previously been reported by Uchino et al. (2017), investigating which waves are present in the innermost open boundary layer. The authors could not directly measure the cold plasma properties due to instrument limitations, and had to instead rely on various assumptions and indirect measurements. Here we confirm with directly measured cold plasma properties that the ion acoustic instability can lead to wave generation during dayside magnetopause reconnection. Furthermore our statistical results show that the ion acoustic instability is likely to be, also in general, responsible for the large amplitude, ion plasma frequency waves often observed by MMS in the magnetospheric separatrix region.

Finally, we present a schematic of the separatrix region (similar to Lindstedt et al. (2009)) in Fig. 4b highlighting the kinetic boundaries, to illustrate the generation of ion acoustic waves during reconnection when cold ions ($T_i < T_e$) are present in the magnetosphere. We show only the southern separatrices, but the same picture holds for the northern separatrices. When reconnection is ongoing the cold plasma in the magnetosphere (i) is convecting (blue arrows) toward the magnetopause. Here, the lack of free energy prevents wavegrowth. As the plasma convects further, it passes the first KAW propagating in the direction of the Alfvén edge out from the ion diffusion region (Vaivads et al., 2010), and its associated current (orange arrows) which has a large field-aligned component. This $j_{\parallel}$ corresponds to a $v_{\parallel}$ shift between electrons and cold ions as seen in (ii). There is thus a positive slope in the electron distribution function, enabling the ion acoustic wave to grow via Landau resonance. Throughout the separatrix region we find both parallel and anti-parallel currents as shown in the example of Fig. 1, intermittently enabling wavegrowth. Field aligned currents are also present in the outflow region (iii), again resulting in Landau resonant growth of ion acoustic waves. As we move deeper into the outflow, the denser and hotter magnetosheath ions start to dominate, leading to Landau damping. This explains why we predominantly see these waves on the magnetospheric side. The end result of this picture is that ion acoustic waves are forming throughout the magnetospheric separatrix region, dissipating parallel currents, and damping KAWs.

5 Conclusions

We investigate the electrostatic, proton plasma frequency waves with $E_\parallel$ amplitudes reaching up to hundreds of mV/m that are frequently found on the magnetospheric side of the magnetopause, often in relation to reconnection events. From dispersion analysis we conclude that the waves are due to an ion acoustic instability between the electrons and cold magnetospheric ions in the separatrix region and near the ion edge. We support this conclusion statistically by analyzing waves from 5 months of MMS data, finding 88% of the waves to be observed when cold ions with thermal energies typically in the range 10-100 eV are present. For 39% of wave observations with cold ions, we compute the cold ion moments and find that cold ions dominate the density $n_{i,\mathrm{cold}}/n_i > 0.6$, and have temperatures lower than the electrons, typically $< 0.4T_e$. This temperature ratio is favourable for ion acoustic waves. Energy for wavegrowth is provided by significant parallel currents. Most of the remaining 61% have similar wave properties and are found during the same magnetopause crossings as some of the 39% mentioned above. This suggests that the ion acoustic instability is responsible for most of the observed waves.

We conclude that these waves are ion acoustic waves formed when cold magnetospheric ions are convected into the separatrix region, where parallel currents drive the plasma unstable to an ion acoustic instability. These waves can be important for separatrix dynamics on both small and large scales. On small scale the waves are capable of trapping cold ions, possibly leading to heating. On larger scales the waves are dissipating parallel currents associated with kinetic Alfvén waves propagating away from the ion diffusion region by reducing the average electron speed to approximately the ion sound speed.

Acknowledgments

We thank the entire MMS team and instrument PIs for data access and support. MMS data are available at https://lasp.colorado.edu/mms/sdc/public/. This work is supported by the Swedish National Space Agency, grant 128/17, and the Swedish Research Council, grant 2016-05507.

References

André, M., & Cully, C. M. (2012). Low-energy ions: A previously hidden solar system particle population. *Geophysical Research Letters*, *39*(3). doi: 10.1029/2011GL050242

Angelopoulos, V. (2008). The THEMIS mission. *Space Science Reviews*, *141*, 5–34. doi: 10.1007/s11214-008-9336-1

Baumjohann, W., & Treumann, R. A. (1996). *Basic space plasma physics.* Imperial College Press.

Birn, J., & Priest, E. R. (2007). *Reconnection of magnetic fields: magnetohydrodynamics and collisionless theory and observations.* Cambridge University Press.

Burch, J. L., Moore, T. E., Torbert, R. B., & Giles, B. L. (2016, March). Magnetospheric Multiscale overview and science objectives. *Space Science Reviews*, *199*(1), 5–21. doi: 10.1007/s11214-015-0164-9

Cowley, S. W. H. (2013). Theoretical perspectives of the magnetopause: A tutorial review. In *Physics of the magnetopause* (p. 29-43). American Geophysical Union (AGU). doi: 10.1029/GM090p0029

Dai, L. (2018). Structures of hall fields in asymmetric magnetic reconnection. *Journal of Geophysical Research: Space Physics*, *123*(9), 7332-7341. doi: 10.1029/2018JA025251

Dai, L., Wang, C., Zhang, Y., Lavraud, B., Burch, J., Pollock, C., & Torbert, R. B. (2017). Kinetic Alfvén wave explanation of the hall fields in magnetic reconnection. *Geophysical Research Letters*, *44*(2), 634-640. doi: 10.1002/2016GL071044

Ergun, R. E., Holmes, J. C., Goodrich, K. A., Wilder, F. D., Stawarz, J. E., Eriksson, S., … André, M. (2016). Magnetospheric Multiscale observations of large-amplitude, parallel, electrostatic waves associated with magnetic reconnection at the magnetopause. *Geophysical Research Letters*, *43*(11), 5626-5634. doi: 10.1002/2016GL068992

Ergun, R. E., Tucker, S., Westfall, J., Goodrich, K. A., Malaspina, D. M., Summers, D., … Cully, C. M. (2016, March). The Axial Double Probe and Fields signal processing for the MMS mission. *Space Science Reviews*, *199*(1-4), 167–188. doi: 10.1007/s11214-014-0115-x

Fairfield, D. H. (1976). Waves in the vicinity of the magnetopause. In B. M. McCormac (Ed.), *Magnetospheric particles and fields* (pp. 67–77). Dordrecht: Springer Netherlands.

Farrell, W. M., Desch, M. D., Kaiser, M. L., & Goetz, K. (2002). The dominance of electron plasma waves near a reconnection x-line region. *Geophysical Research Letters*, *29*(19), 8-1-8-4. doi: 10.1029/2002GL014662

Fried, B. D., & Conte, S. D. (1961). *The plasma dispersion function.* Academic Press, New York.

Gary, S. P., & Omidi, N. (1987). The ion-ion acoustic instability. *Journal of Plasma Physics*, *37*(1), 45–61. doi: 10.1017/S0022377800011983

Gosling, J. T., Thomsen, M. F., Bame, S. J., Onsager, T. G., & Russell, C. T. (1990). The electron edge of low latitude boundary layer during accelerated flow events. *Geophysical Research Letters*, *17*(11), 1833-1836. doi: 10.1029/GL017i011p01833

Graham, D. B., Khotyaintsev, Y. V., Vaivads, A., & André, M. (2015). Electrostatic solitary waves with distinct speeds associated with asymmetric reconnection. *Geophysical Research Letters*, *42*(2), 215-224. doi: 10.1002/2014GL062538

Graham, D. B., Khotyaintsev, Y. V., Vaivads, A., & André, M. (2016). Electrostatic solitary waves and electrostatic waves at the magnetopause. *Journal of Geophysical Research: Space Physics*, *121*(4), 3069-3092. doi: 10.1002/2015JA021527

Graham, D. B., Vaivads, A., Khotyaintsev, Y. V., & André, M. (2016). Whistler emission in the separatrix regions of asymmetric magnetic reconnection. *Journal of Geophysical Research: Space Physics*, *121*(3), 1934-1954. doi: 10.1002/2015JA021239

Gurnett, D. A., Anderson, R. R., Tsurutani, B. T., Smith, E. J., Paschmann, G., Haerendel, G., ... Russell, C. T. (1979). Plasma wave turbulence at the magnetopause: Observations from isee 1 and 2. *Journal of Geophysical Research: Space Physics*, *84*(A12), 7043-7058. doi: 10.1029/JA084iA12p07043

Holmes, J. C., Ergun, R. E., Nakamura, R., Roberts, O., Wilder, F. D., & Newman, D. L. (2019). Structure of electron-scale plasma mixing along the dayside reconnection separatrix. *Journal of Geophysical Research: Space Physics*, *124*(11), 8788-8803. doi: 10.1029/2019JA026974

Huang, H., Yu, Y., Dai, L., & Wang, T. (2018). Kinetic Alfvén waves excited in two-dimensional magnetic reconnection. *Journal of Geophysical Research: Space Physics*, *123*(8), 6655-6669. doi: 10.1029/2017JA025071

Khotyaintsev, Y. V., Graham, D. B., Norgren, C., & Vaivads, A. (2019). Collisionless magnetic reconnection and waves: Progress review. *Frontiers in Astronomy and Space Sciences*, *6*, 70. doi: 10.3389/fspas.2019.00070

Khotyaintsev, Y. V., Vaivads, A., Retinò, A., André, M., Owen, C. J., & Nilsson, H. (2006, Nov). Formation of inner structure of a reconnection separatrix region. *Phys. Rev. Lett.*, *97*, 205003. Retrieved from `https://link.aps.org/doi/10.1103/PhysRevLett.97.205003` doi: 10.1103/PhysRevLett.97.205003

LaBelle, J., Treumann, R. A., Haerendel, G., Bauer, O. H., Paschmann, G., Baumjohann, W., ... Holzworth, R. H. (1987). AMPTE IRM observations of waves associated with flux transfer events in the magnetosphere. *Journal of Geophysical Research: Space Physics*, *92*(A6), 5827-5843. doi: 10.1029/JA092iA06p05827

Lee, J. H., & Angelopoulos, V. (2014). On the presence and properties of cold ions near earth's equatorial magnetosphere. *Journal of Geophysical Research: Space Physics*, *119*(3), 1749-1770. doi: 10.1002/2013JA019305

Li, W. Y., André, M., Khotyaintsev, Y. V., Vaivads, A., Fuselier, S. A., Graham, D. B., ... Burch, J. (2017). Cold ionospheric ions in the magnetic reconnection outflow region. *Journal of Geophysical Research: Space Physics*, *122*(10), 10,194-10,202. doi: 10.1002/2017JA024287

Lindqvist, P.-A., Olsson, G., Torbert, R. B., King, B., Granoff, M., Rau, D., ... Tucker, S. (2016, March). The Spin-Plane Double Probe electric field instrument for MMS. *Space Science Reviews*, *199*(1-4), 137–165. doi: 10.1007/s11214-014-0116-9

Lindstedt, T., Khotyaintsev, Y. V., Vaivads, A., André, M., Fear, R. C., Lavraud, B., ... Owen, C. J. (2009). Separatrix regions of magnetic reconnection at the magnetopause. *Annales Geophysicae*, *27*(10), 4039–4056. doi: 10.5194/angeo-27-4039-2009

Pollock, C., Moore, T., Jacques, A., Burch, J., Gliese, U., Saito, Y., ... Zeuch, M. (2016, March). Fast Plasma Investigation for Magnetospheric Multiscale. *Space Science Reviews*, *199*(1-4), 331–406. doi: 10.1007/s11214-016-0245-4

Russell, C. T., Anderson, B. J., Baumjohann, W., Bromund, K. R., Dearborn, D., Fischer, D., ... Richter, I. (2016, March). The Magnetospheric Multiscale Magnetometers. *Space Science Reviews*, *199*(1-4), 189–256. doi:

10.1007/s11214-014-0057-3

Shay, M. A., Drake, J. F., Eastwood, J. P., & Phan, T. D. (2011, Aug). Super-alfvénic propagation of substorm reconnection signatures and poynting flux. *Phys. Rev. Lett.*, *107*, 065001. Retrieved from `https://link.aps.org/doi/10.1103/PhysRevLett.107.065001` doi: 10.1103/PhysRevLett.107.065001

Stringer, T. E. (1964, jan). Electrostatic instabilities in current-carrying and counterstreaming plasmas. *Journal of Nuclear Energy. Part C, Plasma Physics, Accelerators, Thermonuclear Research*, *6*(3), 267–279. doi: 10.1088/0368-3281/6/3/305

Tang, B.-B., Li, W. Y., Graham, D. B., Rager, A. C., Wang, C., Khotyaintsev, Y. V., ... Burch, J. L. (2019). Crescent-shaped electron distributions at the nonreconnecting magnetopause: Magnetospheric multiscale observations. *Geophysical Research Letters*, *46*(6), 3024-3032. doi: 10.1029/2019GL082231

Toledo-Redondo, S., André, M., Khotyaintsev, Y. V., Lavraud, B., Vaivads, A., Graham, D. B., ... Burch, J. L. (2017). Energy budget and mechanisms of cold ion heating in asymmetric magnetic reconnection. *Journal of Geophysical Research: Space Physics*, *122*(9), 9396-9413. doi: 10.1002/2017JA024553

Uchino, H., Kurita, S., Harada, Y., Machida, S., & Angelopoulos, V. (2017). Waves in the innermost open boundary layer formed by dayside magnetopause reconnection. *Journal of Geophysical Research: Space Physics*, *122*(3), 3291-3307. doi: 10.1002/2016JA023300

Vaivads, A., Khotyaintsev, Y., André, M., Retinò, A., Buchert, S. C., Rogers, B. N., ... Phan, T. D. (2004, Aug). Structure of the magnetic reconnection diffusion region from four-spacecraft observations. *Phys. Rev. Lett.*, *93*, 105001. doi: 10.1103/PhysRevLett.93.105001

Vaivads, A., Retinò, A., Khotyaintsev, Y. V., & André, M. (2010). The Alfvén edge in asymmetric reconnection. *Annales Geophysicae*, *28*(6), 1327–1331. doi: 10.5194/angeo-28-1327-2010

Wilder, F. D., Ergun, R. E., Goodrich, K. A., Goldman, M. V., Newman, D. L., Malaspina, D. M., ... Holmes, J. C. (2016). Observations of whistler mode waves with nonlinear parallel electric fields near the dayside magnetic reconnection separatrix by the magnetospheric multiscale mission. *Geophysical Research Letters*, *43*(12), 5909-5917. doi: 10.1002/2016GL069473

Wilder, F. D., Ergun, R. E., Hoilijoki, S., Webster, J., Argall, M. R., Ahmadi, N., … Giles, B. L. (2019). A survey of plasma waves appearing near dayside magnetopause electron diffusion region events. *Journal of Geophysical Research: Space Physics*, *124*(10), 7837-7849. doi: 10.1029/2019JA027060

Zhou, M., Ashour-Abdalla, M., Berchem, J., Walker, R. J., Liang, H., El-Alaoui, M., … Chandler, M. O. (2016). Observation of high-frequency electrostatic waves in the vicinity of the reconnection ion diffusion region by the spacecraft of the Magnetospheric Multiscale (MMS) mission. *Geophysical Research Letters*, *43*(10), 4808-4815. doi: 10.1002/2016GL069010